

Band-Structure and Many-Body Effects in the Dynamical Response of Aluminum Metal

Andrzej Fleszar,^{1,3} Andrew A. Quong,² and Adolfo G. Eguiluz^{1,3}

¹*Department of Physics and Astronomy, The University of Tennessee, Knoxville, Tennessee 37996-1200*

²*Computational Material Science, Sandia National Laboratory, Livermore, California 94551-0969*

³*Solid State Division, Oak Ridge National Laboratory, Oak Ridge, Tennessee 37831-6032*

(Received 15 July 1994)

For many years, efforts to explain a double peak observed in the dynamical structure factor $S(\mathbf{q}; \omega)$ of aluminum—an archetype of jellium electronic behavior—via inelastic x-ray scattering have concentrated on many-body mechanisms for the uniform electron liquid. On the basis of a first-principles evaluation of $S(\mathbf{q}; \omega)$ for Al crystal we show that the double peak is an intrinsic feature of the response of *noninteracting* electron-hole pairs. Many-electron effects, in the form of a vertex correction for the irreducible polarizability, are found to substantially improve the agreement with experiment of the calculated loss intensities.

PACS numbers: 71.45.Gm

Early inelastic x-ray scattering experiments performed on several metals (Be, Al, Li) [1–4] and on other systems (Si [1] and graphite [1,3]) revealed a then unexpected two-peak structure in the loss spectrum for large wave vectors. Because of the qualitative similarity of the observed spectra (they all show the double peak) for systems with drastically different one-electron band structures [1–5], it was quickly conceded that the periodic crystal potential plays basically no role, i.e., the spectral feature in question was assumed to be a direct manifestation of fundamental physics of the correlated electron liquid—which is why this problem has attracted a large amount of attention [1–15].

Thus, over the past twenty years most theoretical studies [6–13] have addressed the excitation spectra of the above elements in terms of many-body theories of the interacting electron liquid in a uniform compensating background (jellium model). Since the basic mean-field response theory—the random-phase approximation (RPA)—fails to produce the crucial double peak for this model of a metal, the proposed explanations have advocated the importance of various short-range correlation processes. Self-energy effects, such as two-pair excitation and plasmon decay of the quasiparticle states, modeled by a simple lifetime insertion in the propagators, gained initial popularity [6,9,11]. However, the two-peak structure produced by those (in some cases, physically appealing) many-body models has been shown to be spurious [12,13]. The effects of vertex corrections have also been investigated [8,10,11], although estimates of their importance are inconclusive [3,11]. In summary, it seems fair to state that the jellium many-body approaches have failed to provide a consistent explanation for the existence of the double peak.

An opposite, one-electron, viewpoint has been adopted by Schülke *et al.* [4] for the case of Be—an element which, due to its decidedly nonjelliumlike band structure and bonding mechanism, is a prime candidate for the investigation of the effects of the periodic potential [14].

On the basis of a two-band model, these authors have argued that the double peak present in their x-ray data corresponds to electron excitation into final states in a Bragg gap. Such interpretation of the loss spectrum of Be has received support from the recent results of Maddocks, Godby, and Needs [15], who performed an *ab initio* evaluation of the inverse dielectric matrix of this metal within the RPA.

This leaves open the question as to the physics behind the measured dynamical structure factor of Al [5]. Since this element plays such a prototypical role in condensed matter physics, this is a significant question, as it impacts the whole area of dynamical correlations in the electron liquid. In fact, the latest high-resolution synchrotron x-radiation spectra of Al reported recently by Platzman *et al.* [5] were again discussed in terms of jellium many-body theories—because of the long-standing premise that, for this “free-electron metal,” and for the frequencies of interest, i.e., $\omega \geq 2\omega_F$ ($\hbar\omega_F$ being the Fermi energy), the band structure is unlikely to determine the observed physics [5].

In this Letter we report first-principles calculations of the dynamical structure factor of Al which clearly demonstrate that the double peak is built into the noninteracting electron-hole bubble, computed for “real” band electrons. We explicitly identify the excited-state gaps responsible for this effect. Furthermore, we show that the inclusion of a vertex correction for the irreducible polarizability produces a systematic improvement in the quality of the theoretical intensities—for a strong enough vertex [16–18] agreement with experiment [5] is quantitative for all energies. Our results suggest that a systematic x-ray investigation of the dynamical structure factor for wave vectors in the neighborhood of $2k_F$ would be an ideal test of the physics of short-range Coulomb correlations for the electron liquid in *real* metals.

In the first Born approximation, the differential cross section for inelastic scattering of x rays is proportional to the dynamical structure factor $S(\mathbf{q}; \omega)$ —the frequency

and wave vector Fourier transform of the density auto-correlation function for the electrons in the solid. The fluctuation-dissipation theorem [19],

$$S(\mathbf{q}; \omega) = -2\hbar \int d^3x \int d^3x' e^{-i\mathbf{q}\cdot(\mathbf{x}-\mathbf{x}')} \text{Im}\chi_R(\mathbf{x}, \mathbf{x}'; \omega), \quad (1)$$

relates $S(\mathbf{q}; \omega)$ to the imaginary part of the retarded density-response function $\chi_R(\mathbf{x}, \mathbf{x}'; \omega)$, which is a quantity better suited to direct computation. For a periodic crystal we set

$$\chi_R(\mathbf{x}, \mathbf{x}'; \omega) = \frac{1}{\Omega} \sum_{\mathbf{q}} \sum_{\mathbf{G}, \mathbf{G}'} e^{i(\mathbf{q}+\mathbf{G})\cdot\mathbf{x}} e^{-i(\mathbf{q}+\mathbf{G}')\cdot\mathbf{x}'} \chi_{\mathbf{G}, \mathbf{G}'}(\mathbf{q}; \omega), \quad (2)$$

where Ω denotes the normalization volume, \mathbf{G} is a vector of the reciprocal lattice, and $\chi_{\mathbf{G}, \mathbf{G}'}(\mathbf{q}; \omega) \equiv \chi(\mathbf{q} + \mathbf{G}, \mathbf{q} + \mathbf{G}'; \omega)$. Equation (2) allows us to rewrite Eq. (1) in the simpler form

$$S(\mathbf{q}; \omega) = -2\hbar\Omega \text{Im}\chi_{\mathbf{G}=\mathbf{0}, \mathbf{G}'=\mathbf{0}}(\mathbf{q}; \omega), \quad (3)$$

where the wave vector transfer \mathbf{q} can take on arbitrary values—in particular, outside the first Brillouin zone, which is the wave vector domain of interest in the present investigation.

The input to the entire calculation based on Eq. (3) is a well-converged, self-consistent solution for the ground state of the crystal in the local-density approximation (LDA) of density functional theory [20]. Such a solution was constructed by expanding the Kohn-Sham one-electron Bloch states in a plane wave basis with a kinetic-energy cutoff of 12 Ry—the electron-ion interaction being described by a nonlocal, norm-conserving ionic pseudopotential, generated according to the Troullier-Martins scheme [21]. We used the Wigner interpolation formula for local correlation.

The dynamical-response calculations proceed as follows. In addition to the density-response function χ , in the many-body theory of interacting electrons one also introduces an “irreducible polarizability” $\tilde{\chi}(\mathbf{x}, \mathbf{x}'; \omega)$ function which contains the elementary events (electron-hole pair excitation, electron-hole ladders, etc.) from which the response of the ensemble of electrons is built up. This building-up process translates into a Dyson-like integral equation which the exact χ must fulfill [22,23],

$$\chi = \tilde{\chi} + \tilde{\chi}\nu\chi, \quad (4)$$

where ν denotes the bare Coulomb interaction. In the Fourier representation defined by Eq. (2), Eq. (4) becomes a matrix equation for the response coefficients $\chi_{\mathbf{G}, \mathbf{G}'}(\mathbf{q}; \omega)$, from whose knowledge the dynamical structure factor $S(\mathbf{q}; \omega)$ is obtained according to Eq. (3) [24,25].

It is instructive to consider first the $S(\mathbf{q}; \omega)$ which one obtains upon *completely ignoring the Coulomb correlations*, see Fig. 1. To this end we drop the last term in Eq. (4) and replace the exact $\tilde{\chi}$ by its counterpart for noninteracting electrons, i.e., we set $\chi = \tilde{\chi} = \chi^{(0)}$, where

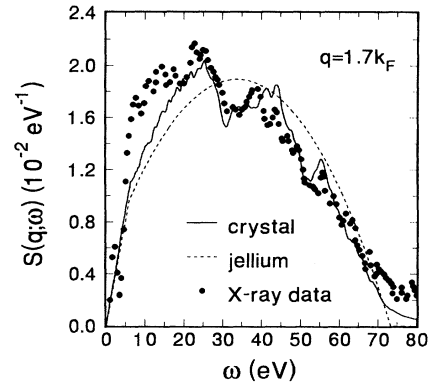


FIG. 1. $S(\mathbf{q}; \omega)$ for noninteracting electron-hole pairs, and its comparison with the x-ray data for Al (Ref. [5]). The solid curve incorporates the band structure of real Al; the dashed curve is for jellium ($r_s = 2.07$). The wave vector transfer \mathbf{q} is along the $(\frac{1}{2}, \frac{3}{2}, 0)$ direction; its magnitude equals $1.7k_F$.

the (retarded) noninteracting electron-hole “bubble” $\chi^{(0)}$ is given by

$$\chi_{\mathbf{G}, \mathbf{G}'}^{(0)}(\mathbf{q}; \omega) = \frac{1}{\Omega} \sum_{\mathbf{k}} \sum_{n, n'} \frac{f_{\mathbf{k}, n} - f_{\mathbf{k}+\mathbf{q}, n'}}{E_{\mathbf{k}, n} - E_{\mathbf{k}+\mathbf{q}, n'} + \hbar(\omega + i\eta)} \times \langle \mathbf{k}, n | e^{-i(\mathbf{q}+\mathbf{G})\cdot\mathbf{x}} | \mathbf{k} + \mathbf{q}, n' \rangle \langle \mathbf{k} + \mathbf{q}, n' | e^{i(\mathbf{q}+\mathbf{G}')\cdot\mathbf{x}} | \mathbf{k}, n \rangle, \quad (5)$$

in which the sums over n and n' run over the band structure for each wave vector \mathbf{k} in the first Brillouin zone, and the $\{f_{\mathbf{k}, n}\}$ are Fermi factors. Now, in a recent paper we reformulated $\chi^{(0)}$ via a Green’s function approach which formally eliminated the need to perform an explicit summation over the unoccupied bands [26]. In the present work we have also used Eq. (5) as it stands, in which case on the order of 40 bands are required for convergence [27].

Figure 1 is striking. *The $S(\mathbf{q}; \omega)$ for (fictitious) noninteracting electron-hole pairs reproduces the main features of the experimental data quite well.* Not only is there a prominent double peak in the theoretical spectrum, but its energy position is rather accurately given, and so are the intensities of the main features. Thus, Fig. 1, in which we also show the corresponding result for jellium—obtained from the well-known Lindhard function—makes it unequivocally clear that the overall two-peak nature of the loss spectrum is an inherent property of $\chi^{(0)}$ for Al *crystal*. [We note that Fig. 1 refers to *exactly* the same \mathbf{q} for which the high-resolution x-ray data of Ref. [5] display a double peak; this wave vector is along the $(\frac{1}{2}, \frac{3}{2}, 0)$ direction.]

This result rules out physical mechanisms previously proposed. First, the *existence* of the double peak has nothing to do with the effects of the electron-electron interaction [1,5–13]—which we have ignored so far. Second, the lower- ω peak in Fig. 1 bears no relationship to a continuation of the plasmon [1,5,11] into the electron-hole

continuum past the wave vector for the onset of Landau damping—the plasmon is absent in the above calculation.

It is useful to visualize in more detail how the process of electron excitation across the Fermi surface—built into $\text{Im}\chi^{(0)}$ —leads to the above result. Figure 2, which for clarity in the presentation refers to a wave vector along the (100) direction ($|\mathbf{q}| = 1.7k_F$), shows the initial- and final-state bands (identified with use of the conservation laws of energy and momentum) which give the most important contribution to Eq. (5) for a given frequency in the vicinity of the dip. Such states lie in planes which are orthogonal to \mathbf{q} and are a distance $|\mathbf{q}|$ apart. Full circles label occupied bands in the (010) direction, and are representative of the dominant initial-state bands. Empty circles identify unoccupied bands whose matrix elements control the numerical value of $\text{Im}\chi^{(0)}$ —those bands correspond to states in the [200] Bragg plane. From Fig. 2 we readily conclude that *the crystal potential opens up an effective excitation gap* for $30 \leq \hbar\omega \leq 40$ eV. The dip in $\text{Im}\chi^{(0)}$ [or $S(\mathbf{q}; \omega)$] for $\hbar\omega \sim 33$ eV is in essence a mapping of this gap. (This conclusion constitutes a multiband, self-consistent generalization of the two-band model of Schülke *et al.* for Be [4].)

The effects of the Coulomb interaction are investigated in Fig. 3, in which (as in Fig. 1) our theoretical spectra are plotted on the same absolute scale as the experimental intensities. At the simplest level we have the RPA, in which, again, $\tilde{\chi} = \chi^{(0)}$, but we now solve Eq. (4)—i.e., the RPA incorporates long-range correlations in χ between the otherwise noninteracting electron-hole pairs which make up $\chi^{(0)}$. The corresponding $S(\mathbf{q}; \omega)$ is seen in Fig. 3 to agree rather poorly with the x-ray data of Platzman *et al.* [5], particularly on the low- ω side of the double peak. Clearly, the RPA *worsens* the quality of the spectrum obtained in Fig. 1 for noninteracting electrons.

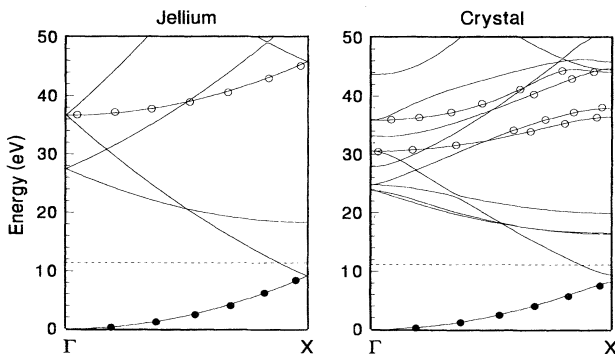


FIG. 2. Relevant portion of the band structure of Al needed in the explanation of the dip in $S(\mathbf{q}; \omega)$. The right (left) panel refers to real Al (jellium with $r_s = 2.07$). With reference to a \mathbf{q} along the (1,0,0) direction, the occupied bands lie on a plane, normal to \mathbf{q} , which basically intersects the zone center; the empty bands lie on the [2,0,0] Bragg plane. See text for details.

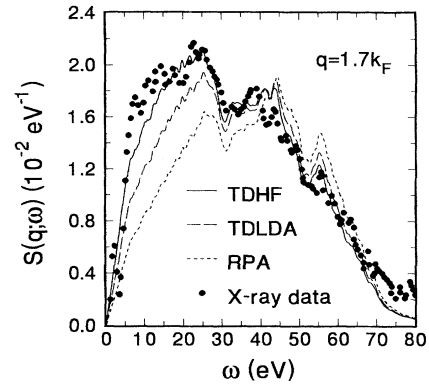


FIG. 3. Comparison of the calculated $S(\mathbf{q}; \omega)$ for Al and the x-ray data of Platzman *et al.* [5]. The wave vector \mathbf{q} is the same as in Fig. 1. The theoretical curves correspond to three different choices for the vertex or local field factor $G(\mathbf{q})$. Intensities are in absolute units. See text for details.

Short-range correlations originate from higher-order diagrams for $\tilde{\chi}$, the RPA ansatz $\tilde{\chi} = \chi^{(0)}$ being of zeroth order in ν . Here we adopt a procedure in the spirit of Hubbard’s original treatment of exchange [22], which leads us to a χ [Eq. (4)] of the symbolic form

$$\chi = \chi^{(0)}[1 - \nu(1 - G)\chi^{(0)}]^{-1}, \quad (6)$$

where the “local-field factor” $G(\mathbf{q})$ (assumed to be static) approximately accounts for the exchange and correlation hole surrounding each electron participating in the screening process ($G = 0$ in the RPA). Alternatively, $f_{xc}(\mathbf{q}) \equiv -\nu(q)G(\mathbf{q})$ represents a “vertex correction” [22].

In Fig. 3 we display the effects of two representative G ’s. First, we have the so-called time-dependent local-density approximation (TDLDA) for χ . In the presence of a weak disturbance from the Kohn-Sham equation in the LDA [20] one readily obtains $G_{\text{TDLDA}}(\mathbf{q}) = -\nu(q)^{-1} \int d^3x e^{-i\mathbf{q}\cdot\mathbf{x}} dV_{xc}(\mathbf{x})/dn(\mathbf{x})$, where $V_{xc}(\mathbf{x})$ is the exchange-correlation potential for the ground-state electron number density $n(\mathbf{x})$. As Fig. 3 illustrates, the TDLDA brings about a substantial improvement over the RPA. Physically, this improvement is due to the approximate TDLDA inclusion of the electron-hole attraction. (For $\hbar\omega \sim 70$ eV the x-ray data show the onset of core excitations, absent in our pseudopotential calculations.)

Now, the TDLDA vertex $f_{\text{TDLDA}}^{xc} = -\nu G_{\text{TDLDA}}$ is only exact for the homogeneous electron liquid for $q \rightarrow 0$ (and for $\omega = 0$). Since this vertex is q independent—a reflection of the local approximation—it ignores the details of the structure of the exchange-correlation hole. The trend apparent in Fig. 3 suggests that the q dependence of the vertex is important, and, furthermore, that a stronger vertex is needed for $|\mathbf{q}| \approx 1.7k_F$. From the myriad of published $G(\mathbf{q})$ ’s we have found that the one obtained by Broens and Devreese [16] from a numerical solution of the time-dependent Hartree-Fock (TDHF) equation for jellium works the best in the present case. Indeed, as Fig. 3

illustrates, the agreement with the x-ray data [5] is now extremely good, for all energies. Numerically, this result is traced to the fact that for the large \mathbf{q} under consideration ($|\mathbf{q}| = 1.7k_F$) we have $G \approx 1$, and thus Eq. (6) yields $\chi \approx \chi^{(0)}$ —i.e., we basically recover the loss spectrum of Fig. 1 for noninteracting electron-hole pairs.

It should be noted that the TDHF vertex, with its prominent spike for $q = 2k_F$, remains a controversial theoretical concept [18]. In particular, this vertex ignores the screening of the ladders for the electron-hole attraction. The remarkable quantitative agreement with experiment which we have just obtained may be due to the fact that for the high frequencies involved (in Al, $\hbar\omega_P \approx 15$ eV) such screening may be ineffective. In any event, our results strongly suggest that the electron-hole vertex manifests itself rather directly in the x-ray data. It would be extremely interesting for a careful experimental investigation of $S(\mathbf{q}; \omega)$ to be performed for Al and other “simple” metals in the neighborhood of $2k_F$. Such a study may help elucidate the physics of short-range correlations in a more direct way than the phonon probe suggested by Overhauser and collaborators [18]. On the theoretical front, the present work provides motivation for a full numerical solution of the integral equation for the irreducible electron-hole vertex in the presence of the actual band structure of Al.

In summary, we have shown that the two-peak structure of the measured $S(\mathbf{q}; \omega)$ for Al is built into the noninteracting electron-hole bubble—i.e., it is not a consequence of Coulomb correlations. However, these correlations play a quantitatively important role. Our results suggest that even for a simple metal such as Al a proper treatment of short-range dynamical electron correlations requires a study of such correlations *for electrons in a lattice*.

We acknowledge useful conversation with E. D. Isaacs. A. A. Q. acknowledges support of DOE, Office of Basic Energy Sciences. A. G. E. acknowledges support from NSF Grant No. DMR-9207747 and the San Diego Supercomputer Center. Oak Ridge National Laboratory is managed by Martin Marietta Energy Systems, Inc., for the Division of Materials Sciences, U.S. DOE under Contract No. DE-AC05-84OR21400.

Note added.—After this paper was submitted, we became aware of a new set of measurements for Al—W. Schülke *et al.*, Phys. Rev. B **47**, 12 426 (1993). (We thank Dr. W. Schülke for bringing this work to our attention.) A detailed comparison with such data will be reported in a subsequent publication.

- [1] P. Eisenberger *et al.*, Phys. Rev. Lett. **31**, 311 (1973); P. M. Platzman and P. Eisenberger, *ibid.* **33**, 152 (1974); P. Eisenberger *et al.*, *ibid.* **34**, 18 (1974); P. Eisenberger and P. M. Platzman, Phys. Rev. B **13**, 934 (1976).
 [2] A. Vratis and G. D. Priftis, Phys. Rev. B **32**, 3556 (1985).

- [3] W. Schülke *et al.*, Phys. Rev. B **33**, 6744 (1986); W. Schülke *et al.*, Phys. Rev. Lett. **59**, 1361 (1987).
 [4] W. Schülke, H. Nagasawa, S. Mourikis, and A. Kaprolat, Phys. Rev. B **40**, 12 215 (1989).
 [5] P. M. Platzman, E. D. Isaacs, H. Williams, P. Zschack, and G. E. Ice, Phys. Rev. B **46**, 12 943 (1992).
 [6] G. Mukhopadhyay, R. K. Kalia, and K. S. Singwi, Phys. Rev. Lett. **34**, 950 (1975).
 [7] A. Holas, P. K. Aravind, and K. S. Singwi, Phys. Rev. B **20**, 4912 (1979); P. K. Aravind *et al.*, *ibid.* **25**, 561 (1982).
 [8] K. Awa *et al.*, Phys. Rev. B **25**, 3670 (1982); **25**, 3687 (1982).
 [9] G. Niklasson, A. Sjölander, and G. Yoshida, J. Phys. Soc. Jpn. **52**, 2140 (1983).
 [10] N. Iwamoto, E. Krotscheck, and D. Pines, Phys. Rev. B **29**, 3936 (1984).
 [11] S. Rahman and G. Vignale, Phys. Rev. B **30**, 6951 (1984).
 [12] T. K. Ng and B. Dabrowski, Phys. Rev. Lett. **33**, 5358 (1986).
 [13] F. Green *et al.*, Phys. Rev. B **31**, 2796 (1985); **35**, 124 (1987).
 [14] M. Taut and W. Hanke, Phys. Status Solidi (b) **77**, 543 (1976).
 [15] N. E. Maddocks, R. W. Godby, and R. J. Needs, Phys. Rev. B **49**, 8502 (1994).
 [16] F. Brosens and J. T. Devreese, Phys. Status Solidi (b) **147**, 173 (1988); F. Brosens *et al.*, Phys. Rev. B **21**, 1363 (1980).
 [17] K. Utsumi and S. Ichimaru, Phys. Rev. B **22**, 5203 (1980); **23**, 3291 (1981).
 [18] Y. R. Wang, M. Ashraf, and A. W. Overhauser, Phys. Rev. B **30**, 5580 (1984); X. Zhu and A. W. Overhauser, *ibid.* **33**, 925 (1986).
 [19] S. Doniach and E. H. Sondheimer, *Green's Functions for Solid State Physicists* (Benjamin, Reading, 1974), Appendix 2.
 [20] W. Kohn and L. J. Sham, Phys. Rev. **140**, A1133 (1965).
 [21] N. Troullier and J. L. Martins, Phys. Rev. B **43**, 1993 (1991).
 [22] G. D. Mahan, *Many-Particle Physics* (Plenum, New York, 1990), 2nd ed.
 [23] Strictly speaking, in diagrammatic perturbation theory Eq. (4) holds for the time-ordered counterparts of the retarded response functions defined in the text.
 [24] We have found the effect of the crystal local fields on $S(\mathbf{q}; \omega)$ —i.e., the effect of the nondiagonal matrix elements of $\chi^{(0)}$ —to be negligible.
 [25] As a check, we have verified the fulfillment of the f -sum rule governing the first-frequency moment of $S(\mathbf{q}; \omega)$; while the x-ray data fulfill this sum rule exactly, our numerical results typically do so within 4% for the \mathbf{q} 's of interest.
 [26] A. A. Quong and A. G. Eguiluz, Phys. Rev. Lett. **70**, 3955 (1993).
 [27] In principle, in Eq. (5) $\eta = 0^+$. The nonzero value of η which we use when sampling the Brillouin zone does not affect our results in any significant way for the large \mathbf{q} 's of interest in this work (typically we used $\eta \approx 0.5$ eV).